Journal of Cellular Physiology

Phosphorylation-Regulated Degradation of the Tumor-Suppressor Form of PED by Chaperone-Mediated Autophagy in Lung Cancer Cells

CRISTINA QUINTAVALLE,[1,2] STEFANIA DI COSTANZO,[1] CIRO ZANCA,[1] IMMACULADA TASSET,[3] ALESSANDRO FRALDI,[4] MARIAROSARIA INCORONATO,[5] PEPPINO MIRABELLI,[5] MARIA MONTI,[6] ANDREA BALLABIO,[4] PIERO PUCCI,[6] ANA MARIA CUERVO,[3] AND GEROLAMA CONDORELLI[1,2]*

[1]*Department of Molecular Medicine and Medical Biotechnology, "Federico II" University of Naples, Naples, Italy*

[2]*Institute of Endocrinology and Experimental Oncology "G. Salvatore" (IEOS), Consiglio Nazionale delle Ricerche (CNR), Naples, Italy*

[3]*Department of Developmental and Molecular Biology, Albert Einstein College of Medicine, New York, New York*

[4]*Telethon Institute of Genetics and Medicine (TIGEM), Naples, Italy*

[5]*IRCCS, SDN Foundation Institute of Diagnostic and Nuclear Development (SDN), Naples, Italy*

[6]*Department of Chemical Science, "Federico II" University of Naples, Naples, Italy*

PED/PEA-15 is a death effector domain (DED) family member with a variety of effects on cell growth and metabolism. To get further insight into the role of PED in cancer, we aimed to find new PED interactors. Using tandem affinity purification, we identified HSC70 (Heat Shock Cognate Protein of 70 kDa)—which, among other processes, is involved in chaperone-mediated autophagy (CMA)—as a PED-interacting protein. We found that PED has two CMA-like motifs (i.e., KFERQ), one of which is located within a phosphorylation site, and demonstrate that PED is a bona fide CMA substrate and the first example in which phosphorylation modifies the ability of HSC70 to access KFERQ-like motifs and target the protein for lysosomal degradation. Phosphorylation of PED switches its function from tumor suppression to tumor promotion, and we show that HSC70 preferentially targets the unphosphorylated form of PED to CMA. Therefore, we propose that the up-regulated CMA activity characteristic of most types of cancer cell enhances oncogenesis by shifting the balance of PED function toward tumor promotion. This mechanism is consistent with the notion of a therapeutic potential for targeting CMA in cancer, as inhibition of this autophagic pathway may help restore a physiological ratio of PED forms.

J. Cell. Physiol. 229: 1359–1368, 2014.

Phosphoprotein enriched in diabetes (PED), known also as phosphoprotein enriched in astrocytes 15 (PEA-15), is a death effector domain (DED) family member with a variety of effects on cell growth and metabolism (Condorelli et al., 1999; Renault et al., 2003). It has a broad anti-apoptotic action, being able to inhibit the intrinsic and the extrinsic apoptotic pathways (Stassi et al., 2005; Garofalo et al., 2008; Zanca et al., 2008; Incoronato et al., 2010). PED is known to interact with a number of proteins, among which are extracellular signal-regulated protein kinases 1 and 2 (ERK1/2), sequestering them in the cytosol and, thus, regulating their function (Formstecher et al., 2001; Romano et al., 2012). PED can be found in an unphosphorylated state, or phosphorylated at Ser104 by protein kinase C, and at Ser116 by AKT or calcium calmodulin kinase II (CamKII) (Trencia et al., 2003; Sulzmaier et al., 2012). Interestingly, PED can act as either a tumor promoter (when phosphorylated) or a tumor suppressor (when unphosphorylated) (Sulzmaier et al., 2012). Moreover, PED has been reported up-regulated in a number of different cancer types, but the mechanisms regulating its expression remain poorly understood (Hao et al., 2001; Stassi et al., 2005; Garofalo et al., 2007; Zanca et al., 2008).

To get further insight into the role of PED in cancer, we have previously reported on the PED interactome identified

Contract grant sponsor: Associazione Italiana Ricerca sul Cancro (AIRC);
Contract grant numbers: 10620, 14046.
Contract grant sponsor: MERIT;
Contract grant number: RBNE08E8CZ_002.
Contract grant sponsor: POR Campania FSE 2007–2013 Project CRÈME.
Contract grant sponsor: Fondazione Berlucchi.
Contract grant sponsor: NIH/NIA;
Contract grant numbers: AG031782, AG03872.
Contract grant sponsor: "Federazione Italiana Ricerca sul Cancro" (FIRC) Post-Doctoral Research Fellowship.
Contract grant sponsor: Fulbright Postdoctoral Fellowship.

*Correspondence to: Gerolama Condorelli, Department of Molecular Medicine and Medical Biotechnology, "Federico II" University of Naples, Via Pansini 5, 80131 Naples, Italy.
E-mail: gecondor@unina.it

Manuscript Received: 23 October 2013
Manuscript Accepted: 27 January 2014

Accepted manuscript online in Wiley Online Library (wileyonlinelibrary.com): 29 January 2014.
DOI: 10.1002/jcp.24569

through tandem affinity purification (TAP) in non-small-cell lung-cancer cells (Zanca et al., 2010): among the interacting proteins found were RAC1 (ras-related C3 botulinum toxin substrate 1), a mammalian rho GTPase protein family member, and HSC70 (heat shock cognate protein of 70 kDa), a chaperone involved in a multitude of housekeeping functions and in chaperone-mediated autophagy (CMA) (Kaushik and Cuervo, 2012a,b). CMA is a uniquely selective form of autophagy in which specific cytosolic proteins are transported one-by-one across the lysosomal membrane for degradation (Massey et al., 2006). This process is constitutively active in many cell types, but it is maximally activated during stress (Kaushik and Cuervo, 2012a). CMA is selective for a subset of soluble cytosolic proteins containing a pentapeptide motif—known as the CMA-targeting motif—biochemically related to Lys-Phe-Glu-Arg-Gln (KFERQ) (Dice, 1990). In the cytosol, HSC70 recognizes the KFERQ sequence present in CMA substrates, and chaperones them to the lysosomal membrane, where they can interact with lysosome-associated protein type 2A (LAMP2A), the CMA receptor. Moreover, HSC70 likely facilitates substrate unfolding, a requirement for substrate translocation across the lysosomal membrane (Kaushik and Cuervo, 2012a,b).

In the present report, we describe the interaction of PED with HSC70, demonstrating that HSC70 targets unphosphorylated PED for CMA. This event has a deleterious effect on cell fate by promoting tumorgenesis.

Materials and Methods

Cell lines and reagents

The human A549 cell line was purchased from American Type Culture Collection (Milan, Italy) and maintained in RPMI medium supplemented with 10% heat-inactivated fetal bovine serum (FBS), 2 mM L-glutamine, and 100 U/ml penicillin–streptomycin. The human embryonic kidney (HEK) 293 cell line was grown in DMEM supplemented with 10% heat-inactivated FBS, 2 mM L-glutamine, and 100 U/ml penicillin–streptomycin. Media, sera, and antibiotics for cell culture were from Sigma–Aldrich (Milan, Italy). Protein electrophoresis reagents were from Bio-Rad (Milan, Italy), and Western blotting and ECL reagents were from GE Healthcare (Milan, Italy). HSC70 antibody was from Santa Cruz Biotechnology (Santa Cruz, CA), human LAMP2A antibody was from Abcam (MA), β-actin antibody was from Sigma–Aldrich, and Myc antibody was from Cell Signaling Technology (Milan, Italy). The PED antibody was generated as described before (Condorelli et al., 2002). For transfection, Lipofectamine 2000 was purchased from Life Technologies (Milan, Italy). The plasmids used encoded Myc–PED (Condorelli et al., 1998) and the phosphorylation mutants HA-PED-S104/116^{A} and HA-PED-S104/116^{D} (a kind gift from Dr Mark H. Ginsberg, The Scripps Research Institute, La Jolla, San Diego, CA); Lamp2a shRNA and Lamp2a cDNA were from Dr Ana Maria Cuervo (Massey et al., 2006);) siRNA for Hsc70 was from Santa Cruz Biotechnology. Cloroquine and NH_4Cl were from Sigma–Aldrich. All the chemicals used for the in vitro lysosome experiments have been described previously (Cuervo et al., 1994).

Immunoprecipitation

HEK293 cells were cultured at 90% final confluence in p100 plates. After 24 h, cells were transfected with 8 μg of plasmids using Lipofectamine 2000. Forty-eight hours later, the cells were harvested with RIPA buffer (0.15 mM NaCl, 0.05 mM Tris–HCl, pH 7.5, 1% Triton, 0.1% SDS, 0.1% sodium deoxycolate, 1% Nonidet P40, and 1× protease and phosphatase inhibitor cocktail) on a shaker for 30 min, and 1 mg of total extract immunoprecipitated with 4 mg/ml PED antibody or a 1:1,000 dilution of Myc antibody for 16 h on a shaker. A/G beads (Santa Cruz Biotechnology) were then added for 2 h, after which the beads were washed three times with washing buffer (50 mM Tris–HCl pH 7.5, 150 mM NaCl, 0.1% Triton, 10% glycerol), 30 μl of sample buffer added, and the samples boiled at 100°C for 5 min. The supernatants were resolved on 12% polyacrylamide gels by SDS–PAGE.

Western blotting

Total proteins from A549 and HEK293 cells were extracted with RIPA buffer. Fifty micrograms of sample extract were resolved on 10–15% SDS–polyacrylamide gels using a mini-gel apparatus (Bio-Rad Laboratories, Richmond, CA) and transferred to Hybond-C extra nitrocellulose (GE Healthcare, Milan, Italy). Membranes were blocked for 1 h with 5% non-fat dry milk in TBS–0.05% Tween-20, incubated overnight with primary antibody, washed, incubated for 1 h with secondary antibody, and visualized by chemiluminescence.

Immunofluorescence

A549 cells were serum starved for 24 h before analysis. To enhance the lysosomal localization and to prevent degradation, bafilomycin A (Sigma–Aldrich) was added to serum-depleted media. Cells were fixed with 4% paraformaldehyde for 10 min, permeabilized with Triton 0.1% in PBS for 10 min at room temperature, and blocked in 10% FBS–0.1 % saponin in PBS. Primary antibodies were dissolved in 1:10-diluted blocking solution and incubated at the following dilutions for 1 h at room temperature: anti-PED, 1:100; anti-HSC70, 1:100; anti-LAMP2A, 1:200. Cells were then incubated for 1 h at room temperature as appropriate with an anti-rabbit green fluorochrome antibody (Alexa 488-conjugated phalloidin), an anti-rabbit red fluorochrome antibody (Alexa 594), or an anti-mouse red fluorochrome antibody (Alexa 459), all purchased from BD Bioscience (Milan, Italy) and diluted 1:1,000 in 1:10-diluted blocking solution. Cells were then washed four times in cold PBS. Antigen–antibody complexes were visualized by confocal microscopy under a Zeiss LSM 510 microscope equipped with a Zeiss confocal-scanning laser and a 1.4 objective with a 60× numerical aperture.

Quantification of cell viability

Cells were seeded in 96-well plates in triplicate and incubated at 37°C in a 5% CO_2 incubator. SuperKiller TRAIL was used at a final concentration of 50 ng/ml for 24 h. Cell viability was evaluated with the CellTiter 96 AQueous One Solution Cell Proliferation Assay (Promega, Milan, Italy), according to the manufacturer's protocol. Metabolically active cells were detected by adding 20 μl of MTS to each well. After 2 h of incubation, plates were analyzed in a Multilabel Counter (BioTek, Milan, Italy).

Recombinant PED protein production

BL21 cells were transformed with a glutathione-S-transferase (GST)–PED vector. The cells were induced with 0.5 mM IPTG (Qiagen, Milan, Italy) for 4 h, harvested, resuspended in PBS, and then sonicated. 1% Triton X-100 was added at a final concentration of 0.1% and the cells were left for 30 min in agitation on a wheel at 4°C. Lysates were then centrifuged at 12,000*g* for 10 min at 4°C and then loaded onto a polyacrylamide analytic gel. GST-tagged protein was isolated using GSTrap HP columns (GE Healthcare, Milan, Italy) according to manufacturer's instructions. Briefly, columns were equilibrated with cold 1× PBS, and lysate pumped onto the columns. After five washings with 1× PBS, tagged protein was eluted with 1 ml elution buffer (50 mM Tris-HCl, 10 mM reduced glutathione, pH 8.0). Eluted protein was aliquoted and stored at −80°C. The purified GST–PED recombinant protein was analyzed by staining of SDS–PAGE gels with Sypro-Ruby protein gel stain (Life Technologies, Milan, Italy). We observed a ~37 kDa band relative to purified GST-PED recombinant protein

and an aspecific lower second band that remains constant and therefore not related to PED expression (Supplementary Fig. 1A).

GST pull-down assay

Cells were cultured at a final concentration of 90% in p100 plates. After a quick wash with ice-cold PBS, cells were lysed with GST–Fish buffer (50 mM Tris–HCl pH 7.4, 2 mM $MgCl_2$, 1% NP-40, 10% glycerol, 100 mM NaCl, 1 mg/ml leupeptin, 1 mg/ml pepstatin, 1 mg/ml aprotinin, 1 mM PMSF, and 2 mM DTT). The lysates were cleared by centrifugation in a pre-cooled rotor. One hundred fifty micrograms of total protein extract was mixed with 10 or 20 μg of GST–PED recombinant protein coupled to glutathione–sepharose beads and incubated 30 min at 4°C with agitation. Beads were then rapidly rinsed three times with 1 ml of ice-cold GST–Fish buffer (Zanca et al., 2010). Total HSC70 was estimated by immunoblotting.

Animals

Adult male Wistar rats (Charles River Laboratories, Milan, Italy) with a body weight of 200–250 g were fasted for 48 h before sacrifice and removal of livers. Rats were treated and euthanized in compliance with the Albert Einstein College of Medicine institutional guidelines and protocols. Approval for the experimentation was received from the institution's Animal Care and Use Committee.

Lysosomal isolation

The method used has been described previously (Cuervo et al., 1997). Briefly, fasted Wistar rats were anesthetized with ether and then decapitated. Liver homogenates were centrifuged at 2,500*g* for 10 min on 7 ml chilled 0.25 M sucrose/*g* of tissue, and then the supernatant centrifuged at 6,800*g* for 25 min. After resuspension and washing once, the sediment (mitochondrial–lysosomal fraction) was loaded on the bottom of a discontinuous metrizamide gradient (Nycomed, Oslo, Norway) and centrifuged for 2 h. Fractions 1 and 2 were collected from the gradient, diluted five times with 0.3 M sucrose, and lysosomes sedimented at 37,000*g* for 10 min. Lysosomal integrity was verified after isolation by measuring β-hexosaminidase latency (Storrie and Madden, 1990), and only preparations with >95% intact lysosomes were used.

Measurement of CMA activity

Freshly isolated rat liver lysosomes that had been either left untreated or treated with protease inhibitors for 10 min at 0°C were incubated with recombinant PED, ovalbumin, or glyceraldehyde-3-phosphate dehydrogenase (GAPDH) in 10 mM 3-(N-morpholino) propanesulfonic acid (MOPS) buffer (pH 7.3) and 0.3 M sucrose for 20 min at 37°C (Kaushik and Cuervo, 2009). Lysosomes were then collected by centrifugation, subjected to

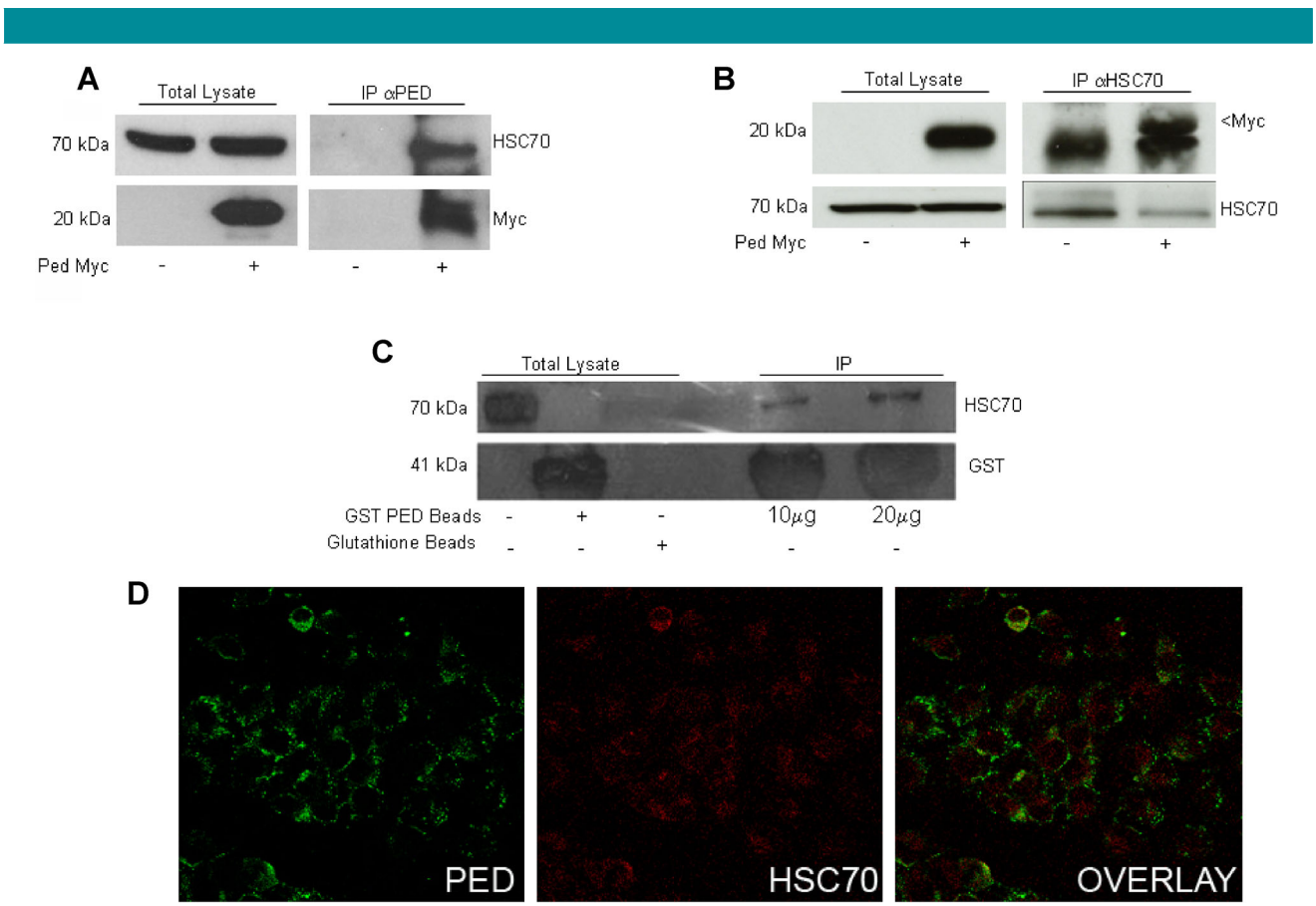

Fig. 1. Validation of PED–HSC70 interaction. A,B: Representative immunoprecipitation experiments on HEK293 cells transfected with Myc–PED cDNA. After 48 h, 1 mg of protein extracts were immunoprecipitated with anti-PED (A), anti-HSC70 (B), or control IgG, as indicated. C: Representative GST pull-down experiment. A549 cell extracts were incubated with two amounts of glutathione–sepharose 4B beads pre-bound to GST–PED fusion protein. The negative control was obtained by incubating cellular extracts with beads not pre-bound to GST–PED; pre-bound GST–PED fusion beads (10 μg) were used as the positive control. Fifty micrograms of total cellular extract was loaded. D: representative confocal experiments. The distribution of PED and HSC70 in A549 cells was determined with confocal microscopy. The intensity of the yellow immunofluorescence signal represents the degree of co-localization of the two proteins. We observed an 18.5% overlay of the two signals.

SDS–PAGE, and immunoblotted. Uptake was calculated as the difference between the amount of substrate associated with lysosomes (protease inhibitor-treated lysosomes) and the amount of substrate bound to their membrane (untreated lysosomes).

Statistical analysis

Student's *t*-test was used to analyze the differences between values. A probability level <0.05 was considered significant. Data were analyzed with GraphPad Prism for Windows (San Diego, CA). Quantification was obtained with ImageJ for Windows (http://rsb.info.nih.gov). Immunofluorescence co-localization signals were obtained with ImageJ plugins, considering ~35 cells/image of three different acquisitions.

Results

PED interacts with HSC70

Using TAP (Zanca et al., 2010), we identified an interaction between HSC70 and PED. That finding was confirmed by three other approaches (Fig. 1): co-immunoprecipitation, GST fusion protein pull-down, and confocal microscopy. For the co-immunoprecipitation experiment, A549 cells—an adenocarcinomic human alveolar basal epithelial cell line—were transfected with Myc–PED cDNA, the cell extract immunoprecipitated with anti-PED, and the interaction revealed by Western blotting with anti-HSC70 (Fig. 1A); in addition, some samples were immunoprecipitated with anti-HSC70 and then blotted for Myc (Fig. 1B). In both experimental settings, HSC70 co-immunoprecipitated with PED. We then assessed the direct binding of PED with HSC70 in A549 cell extracts incubated with different quantities of a recombinant GST–PED fusion protein or, as a negative control, with glutathione–sepharose 4B beads not pre-bound to the recombinant protein. We found that HSC70 was pulled down by the GST-PED recombinant protein in a dose-dependent manner (Fig. 1C). Finally, we observed clear PED–HSC70 co-localization with confocal microscopy: co-localization of the immunofluorescence signals occurred mostly in the cytosol, although it was also present in punctate structures suggestive of intracellular vesicles (Fig. 1D).

PED–HSC70 interaction and CMA

Next, we assessed whether PED's association with HSC70 was at least in part due to its targeting for CMA. For this purpose,

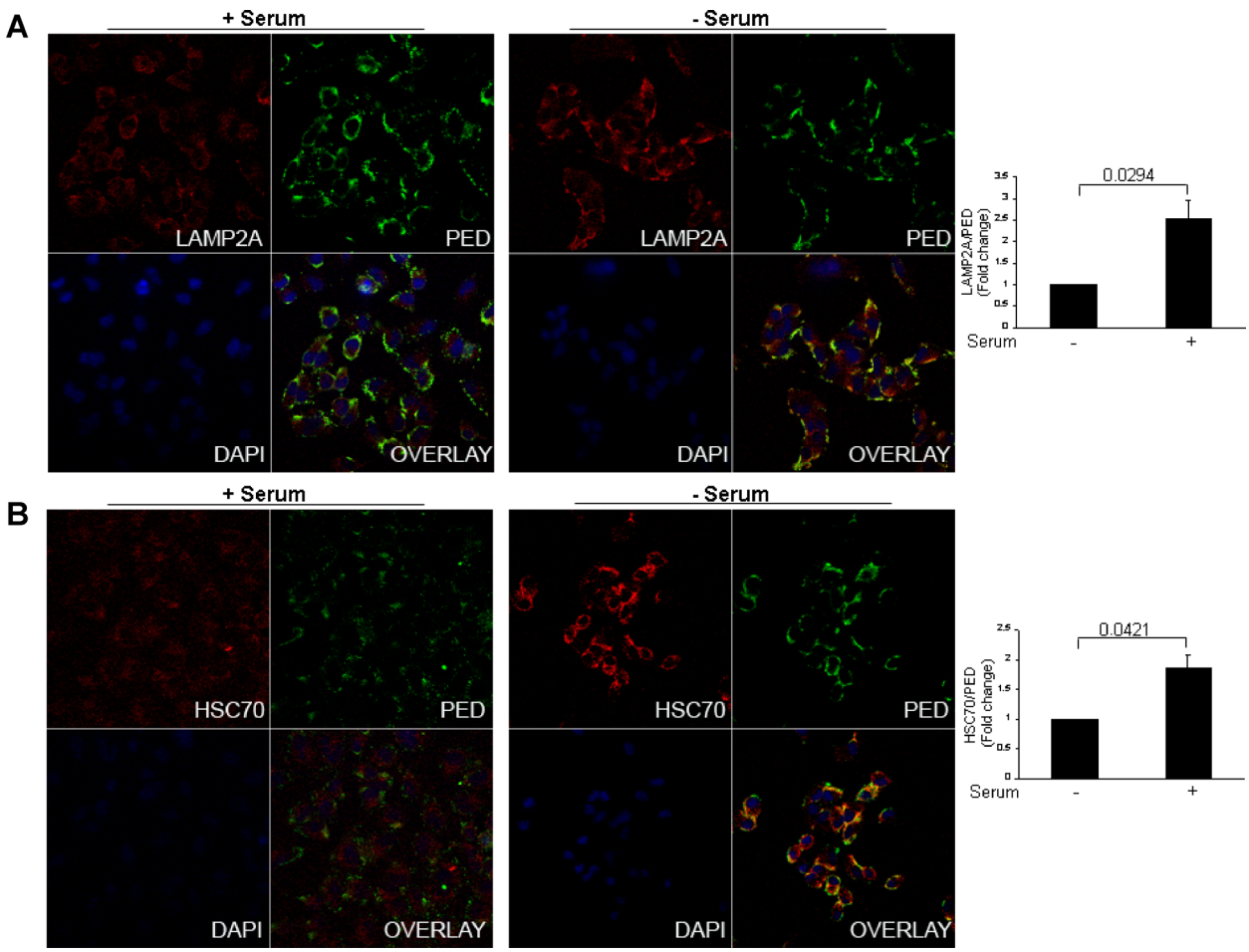

Fig. 2. PED localizes to CMA-associated lysosomes. A: Cellular localization of PED (green) and LAMP2A (red) in A549 cells cultured with (+) or without (−) serum. DAPI was used to stain nuclei. The graph on the right gives relative quantitative analysis of PED/LAMP2A co-localization. Serum starvation, which enhances CMA, was associated with increased signal co-localization, indicative of PED localizing to CMA-associated lysosomes. Means + standard deviations; statistical analysis is Student's *t*-test. B: Cellular localization of PED (green) and HSC70 (red) in A549 cells cultured with and without serum. The graph on the right gives relative quantitative analysis of PED/HSC70 co-localization. Again, signal co-localization was increased in serum-starved cells. Means + standard deviations; statistical analysis is Student's *t*-test.

A549 cells were cultured either in the presence of serum, a condition resulting in low CMA, or with prolonged (24 h) serum starvation, a setting in which CMA is enhanced (Cuervo et al., 1997), we evaluated the intracellular distribution of PED and its co-localization with HSC70- and LAMP2A-positive lysosomes with confocal microscopy. As expected, serum starvation up-regulated CMA, with CMA-associated lysosomes, that is, those enriched in LAMP2A (Supplementary Fig. 2A) and HSC70 (Supplementary Fig. 2B), clearly relocating to the perinuclear region (Kaushik and Cuervo, 2009), and with the co-localization of HSC70 and LAMP2A significantly increasing within vesicular structures (Supplementary Fig. 2B). PED also co-localized with LAMP2A (Fig. 2A) and HSC70 (Fig. 2B), especially when CMA activity was stimulated by serum starvation.

Uptake of PED in ex vivo lysosomes

The most direct way to determine if a protein is a CMA substrate is to reproduce its direct translocation into isolated lysosomes (Cuervo et al., 1997; Kaushik and Cuervo, 2009). Therefore, we incubated intact ex vivo rat liver lysosomes with purified recombinant GST–PED protein and determined lysosomal uptake by comparing the amounts of PED associated with lysosomes previously treated or not with protease inhibitors. We found that a fraction of PED was associated with lysosomes and that the amount increased with protease inhibition, confirming that PED accumulates within lysosomes (Fig. 3A,B). The same behavior was observed for other well-characterized CMA substrates, like ribonuclease A, GAPDH (Cuervo et al., 1994), and tau protein, but was not observed for cyclophilin A, which is not a substrate for CMA (Fig. 3A). The accumulation of PED in lysosomes was saturable (Fig. 3C).

To further confirm that internalization of PED within lysosomes was due to CMA, we compared the effect that other proteins had on PED uptake. Ovalbumin—a protein lacking any KFERQ-like motif and reported not to undergo CMA (Cuervo et al., 1994)did not have any effect on the amount of PED associated with lysosomes; in contrast, GAPDH was able to partially reduce PED uptake, indicating competition for components of the CMA machinery (Fig. 3D). This competition between PED and other CMA degradable proteins was reciprocal, since increasing concentrations of one gradually decreased the amount associated with lysosomes of the other (Fig. 3E). These findings support the notion that PED is a *bona fide* CMA substrate, since it can be internalized directly into

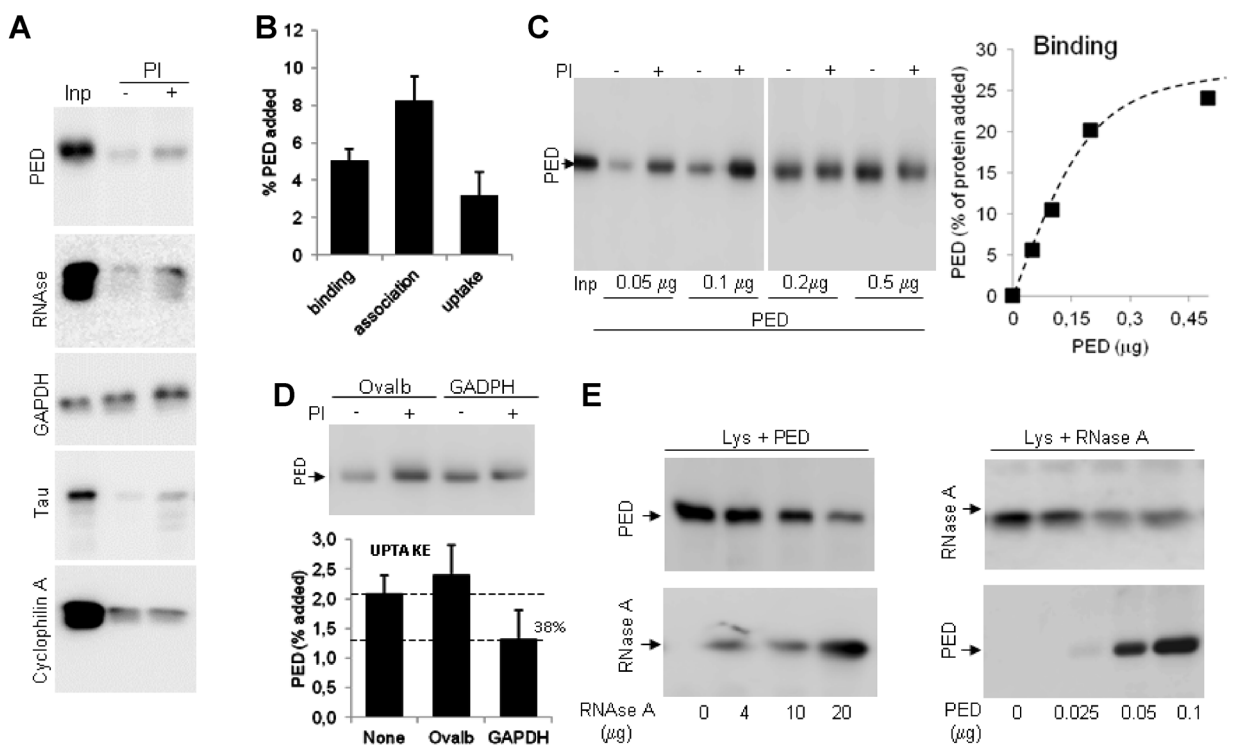

Fig. 3. Uptake of PED by lysosomes via chaperone-mediated autophagy. A: Intact ex vivo rat liver lysosomes were pretreated (+) or not (−) with protease inhibitors (PI) and then incubated with either purified GST–PED, a known CMA substrate (i.e., ribonuclease A: RNase; glyceraldehyde 3 phosphate dehydrogenase: GAPDH; tau protein: Tau), or a non-CMA substrate protein (cyclophillyn A: CycA). Lysosomes were collected by centrifugation and subjected to SDS–PAGE and immunoblotting. In: input. B: Quantification of the association of PED with lysosomes. Values are expressed as a percentage of the protein added (0.1 mg), calculated as described in the Material and Methods section. Means + standard errors of n = 4 experiments. C: Lysosomes were incubated with increasing amounts of GST–PED and processed as in (A). Representative immunoblot (left) and quantification of the percentage of PED accumulated within lysosomes (right). In: input; + and −: respectively, lysosomes incubated with and without protease inhibitors. D: Lysosomes that had been pretreated (+) or not (−) with protease inhibitors were incubated with PED in the presence of GAPDH or ovalbumin (OVA), respectively a CMA and a non-CMA substrate, and processed as in (A). Representative immunoblot (top). Quantification (bottom) indicated that lysosomal uptake of PED was reduced 38% in the presence of GAPDH. Values are means + standard errors of n = 4 experiments. E: Lysosomes were incubated with a fix concentration of PED and then increasing concentrations of RNase A (left) or with a fixed amount of RNase A and then increasing concentrations of PED (right). As can be seen from the representative immunoblots, competition for lysosomal uptake was reciprocal.

isolated lysosomes using similar mechanisms to those described for other CMA-degraded proteins (Cuervo et al., 1994; Salvador et al., 2000).

PED level is regulated by lysosomal activity

We then tested whether the modulation of lysosome activity in intact cells could affect the intracellular levels of PED. To this end, CMA was activated or inhibited in A549 cells and intracellular PED levels then assessed. To activate CMA, cells were incubated in serum-deprived medium or transfected with LAMP2A cDNA, the protein limiting CMA (Cuervo and Dice, 2000). In both settings, the intracellular level of PED decreased (Fig. 4A). Coherently, when CMA was inhibited with chloroquine—an inhibitor of lysosome-mediated degradation for all types of autophagy—or with Lamp2a shRNA or HSC70 RNAi, intracellular PED increased (Fig. 4B). Moreover, induction/inhibition of CMA modulated the level of exogenous PED (Fig. 4C). Thus, a part of cellular PED normally undergoes degradation in lysosomes via CMA.

Role of phosphorylation in CMA-mediated PED degradation

The KFERQ motif consists of a glutamine preceded or followed by a basic (lysine/arginine; represented with a +), an acidic (aspartic acid/glutamic acid; represented with a −), a bulky hydrophobic (phenylalanine/isoleucine/leucine/valine; represented with φ), and then a repeated basic or bulky hydrophobic amino acid. A small number of peptides will have the glutamine substituted by the related amino acid asparagine (Dice, 1990; Majeski and Fred Dice, 2004). The analysis of PED's amino acid sequence revealed the presence of two possible CMA-targeting motifs: NKLDK (amino acids 52–57; N+φ−+), and DIIRQ (amino acids 110–115; −φφ+Q) (Fig. 5A). The latter motif resides close to two major PED

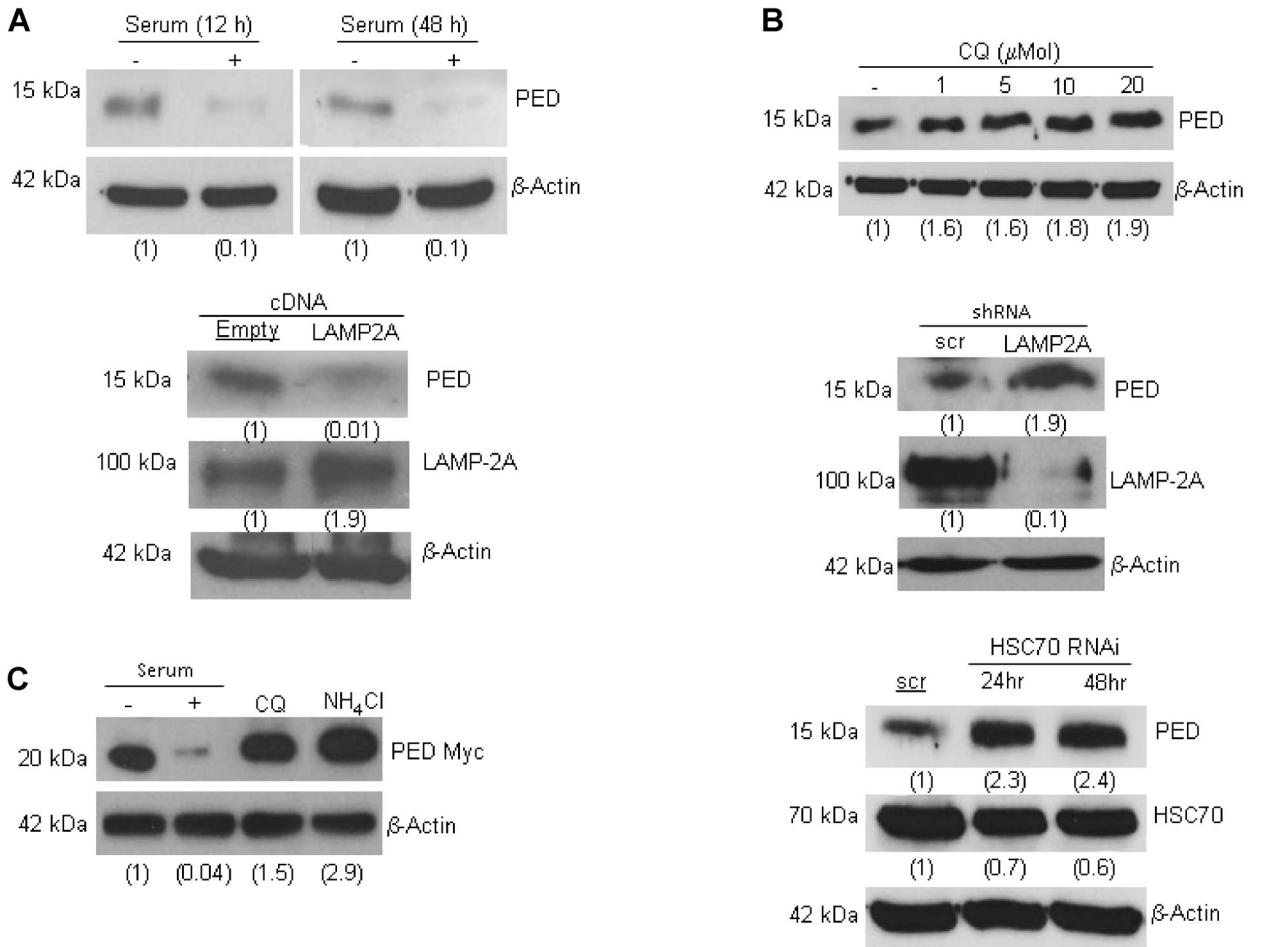

Fig. 4. PED expression is affected by CMA activity. A: CMA was activated in A549 cells by either 12 or 24 h of serum starvation (top panel) or by transfection with Lamp2a cDNA (bottom panel). Incubation with serum or an empty vector were used as controls. Western blotting revealed that the intracellular level of PED decreased when CMA was activated. Representative blots are shown. The numbers in brackets indicate optical density of the bands, arbitrarily set to 1 for the negative control lysate. B: Inhibition of CMA with increasing doses of chloroqiuine (CQ), a lysosomal inhibitor (top-most panel), increased intracellular PED, as did intervention on the CMA-associated proteins LAMP2A (middle panel) and HSC70 (bottom-most panel) with short hairpin RNA (shRNA) and RNA interference (RNAi). Scrambled sequences (Scr) were used for control experiments. The numbers in brackets indicate optical density of the bands, arbitrarily set to 1 for the negative control lysate. C: A549 cells were transfected for 24 h with Myc–PED cDNA and then serum deprived or treated with 10 μM chloroquine (CQ) for 24 h or 15 mM ammonium chloride (NH_4Cl) for 4 h. PED levels were then assessed by Western blot. The numbers in brackets indicate optical density of the bands, arbitrarily set to 1 for the PED-Myc lysate.

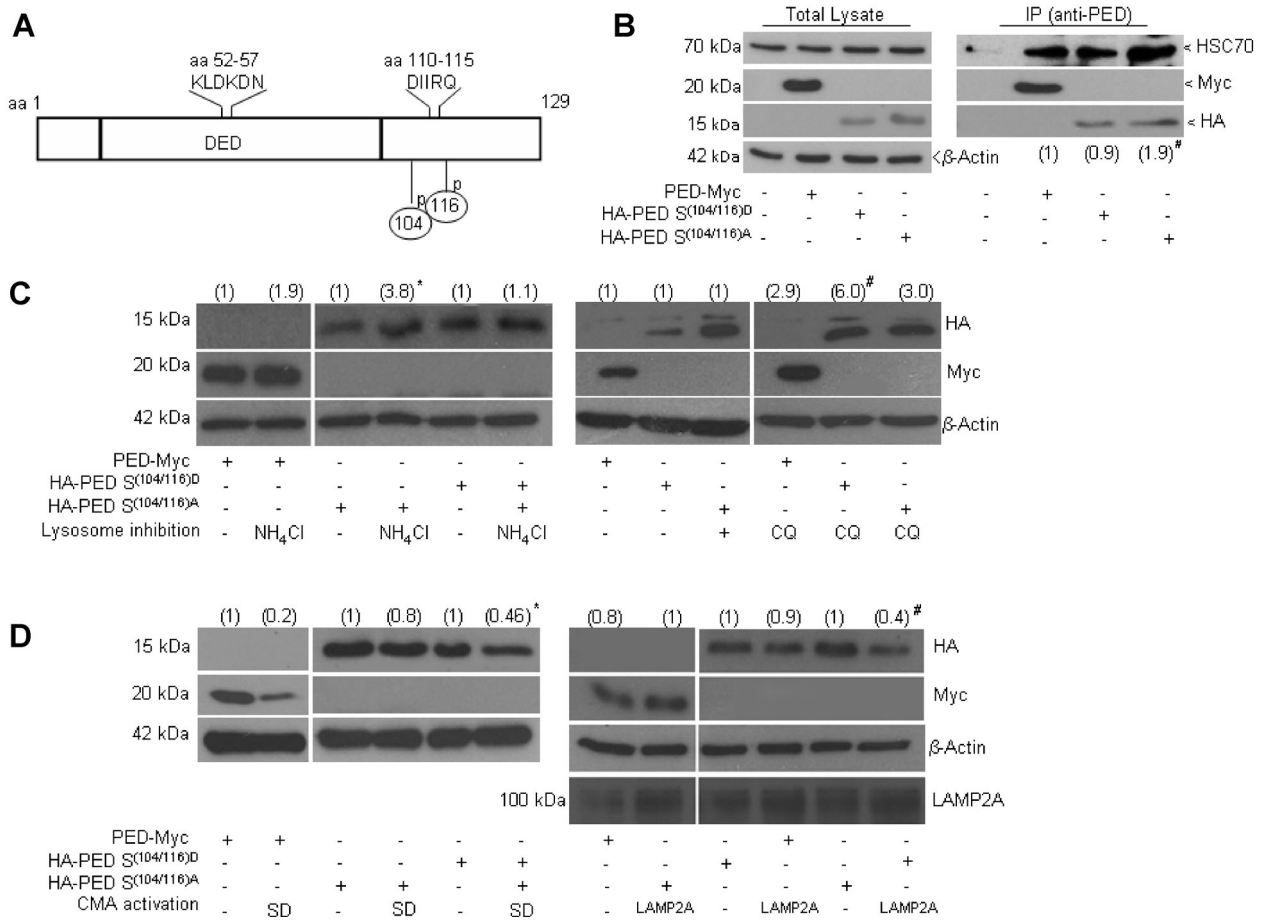

Fig. 5. CMA degrades unphosphorylated PED. A: Schematic representation of the PED protein, showing phosphorylation and putative KFEQR sites. B: HEK293 cells were transfected with cDNA for Myc–PED (wild-type PED), HA-PED-S104/116^{A} (a phosphorylation-dead form of PED), or HA-PED-S104/116^{D} (a phosphorylated-PED mimic). After 48 h, 1 mg of protein extracts were immunoprecipitated with anti-PED or control IgG, resolved with SDS–PAGE, and then Western blotted. The numbers in brackets indicate optical density of the HSC70 bands, arbitrarily set to 1 for the Myc-PED lysate; HA-PED-S104/116^{D} versus HA-PED-S104/11^{A}, *P*-value <0.03. C: A549 cells were transfected as in B and lysosomes inhibited with either 15 mM of NH_4Cl for 4 h or 10 μM of chloroquine (CQ) for 24 h. The numbers in brackets indicate optical densities of the HA or Myc bands, arbitrarily set to 1 for control lanes; *$P < 0.03$ (vs. HA-PED-S104/116^{D}); #$P < 0.04$ (versus HA-PED-S104/116^{D}). D: A549 cells were transfected as in B and CMA activated either by serum deprivation (SD) for 24 h or overexpression of LAMP2A via transduction with a cDNA (LAMP2A). The numbers in brackets indicate optical densities of the HA or Myc bands, arbitrarily set to 1 for control lanes; *$P < 0.04$ versus HA-PED-S104/116^{D}; #$P < 0.03$ versus HA-PED-S104/116^{D}.

phosphorylation sites — Ser114 and Ser116 (Condorelli et al., 2002; Trencia et al., 2003; Stassi et al., 2005). Therefore, we tested whether PED phosphorylation affected its interaction with HSC70 and, hence, its degradation via CMA. For this purpose, we transfected HEK293 cells with either a phosphomimic PED mutant in which Ser104/116 were substituted with aspartic acids (HA-PED-S104/116^{D}), or with a phosphorylation-dead mutant in which Ser104/116 were substituted with alanines (HA-PED-S104/116^{A}) (Krueger et al., 2005; Sulzmaier et al., 2012). We found that PED-S104/116^{A} interacted with HSC70 almost twofold more than did PED-S104/116^{D} (Fig. 5B). Therefore, changes in PED phosphorylation state modify its amenability for lysosomal degradation. Coherently, when lysosomal degradation was inhibited with either NH_4Cl or chloroquine, wild-type PED and PED-S104/116^{A} accumulated, whereas PED-S104/116^{D} levels remained unchanged (Fig. 5C).

To prove that the findings were related to CMA, we induced CMA with either serum starvation or overexpression of LAMP2A with a cDNA. We found that up-regulation of CMA resulted in a more pronounced decrease in the level of PED-S104/116^{A} than of wild-type PED, indicative of increased degradation of PED when unphosphorylated; in contrast, levels of PED-S104/116^{D} remained unchanged upon CMA up-regulation (Fig. 5D), consistent with a failure to undergo degradation via this pathway when PED is phosphorylated.

Physiological relevance of CMA for PED function

The main activity of PED, in non-small-cell lung carcinoma above all, is the regulation of cell apoptosis/viability (Condorelli et al., 1999, 2002; Renault et al., 2003; Zanca et al., 2008). Therefore, we investigated the effect of PED mutants during CMA, on cell viability and apoptosis. To this end, we activated CMA with serum starvation and then verified cell viability and response to tumor necrosis factor-related apoptosis-inducing ligand (TRAIL)-induced apoptosis in A549 cells overexpressing either the phosphomimic or the phosphorylation-dead mutant.

We found that the phosphomimic PED mutant conferred a growth advantage (Fig. 6A) and increased resistance to TRAIL-induced apoptosis (Fig. 6B).

Discussion

Here, we identify PED as a new substrate of chaperone-mediated autophagy. We identified two KFERQ-like motifs in the amino acid sequence of PED, one of which is located within a previously described phosphorylation site. Although it is clear that the chaperone protein HSC70 can recognize the KFERQ motif, little is known on how this process is modulated. Protein folding-unfolding may be important for recognition (Kaushik and Cuervo, 2012a), so if the KFERQ motif is present in the protein's core, the binding of HSC70 may occur only when the protein unfolds. In other proteins, the motif may be masked by protein–protein interaction. Very little is known on the effect of post-translational modification on the ability of HSC70 to recognize CMA-targeting motifs. Acetylation is the only post-translational modification described to date to modulate CMA of a protein (Lv et al., 2011). PED is the first example where phosphorylation modifies the ability of HSC70 to access KFERQ-like motifs.

PED phosphorylation occurs on two serine residues: Ser104, a PKC target (Krueger et al., 2005), and Ser116, which is targeted by CaMKII and AKT (Condorelli et al., 2002; Trencia et al., 2003; Sulzmaier et al., 2012). Several reports suggest that PED phosphorylation is determinant for its functions: phosphorylation leads to a tumor-promoting effect through increased proliferation and inhibition of apoptosis, whereas dephosphorylation allows PED to bind ERK1/2, leading to a tumor suppressing effect through blockade of nuclear translocation and cellular proliferation (Formstecher et al., 2001). Phosphorylation of Ser116 regulates the anti-apoptotic function of PED and modulates its targeting to the death-inducing signaling complex (Condorelli et al., 1999; Trencia et al., 2003). Several findings support the idea that PED may have a dual pro-survival/tumorigenic function in many types of neoplasm, such as skin, breast, ovarian, and lung cancer, and glioblastoma, while being tumor-suppressive in other types (Lee et al., 2012; Funke et al., 2013). Thus, PED phosphorylation status is very important for cell fate. Most emphasis has been placed in the identification of the kinases that contribute to the switch from an anti- to a pro-oncogenic function by actively phosphorylating PED. For example, PED function is regulated by HSP27 through modulation of Akt activity and stability (Hayashi et al., 2012). However, the contribution of other cellular processes to the modulation of this switch has not been previously explored. In this report, we show for the first time that changes in the balance of PED phosphorylation is mediated by degradation via CMA.

We have observed that PED is up-regulated in lung cancer, and its expression correlates with histological grade and apoptosis resistance (Zanca et al., 2008; Incoronato et al., 2010, 2011). PED might be up-regulated in cancer cells to compensate for its faster degradation due to the up-regulation of CMA, which recent reports have described as being up-regulated, in particular, in lung cancer (Kon et al., 2011). However, a more attractive explanation is that the up-regulation of CMA observed in this type of cancer (Kon et al., 2011) may contribute to further imbalance between the pro- and anti-oncogenic forms of PED by removal of the subset of PED having an inhibitory effect on tumorigenesis. Indeed, as reported here, non-phosphorylated PED, in contrast to the phosphorylated protein, is readily delivered for CMA degradation (Fig. 7). Therefore, we speculate that the up-regulation of CMA inherent in lung cancer may preferentially degrade the tumor-suppressor form of PED, contributing in this way to tumor progression. Further studies will aim to elucidate whether the anti-oncogenic effect of blocking CMA in cancer cells (Kon et al., 2011) is obtained, at least in part, through an increase in the amount of the anti-oncogenic PED.

Although the mechanism described here mainly refers to CMA-mediated autophagy, it is worth highlighting that PED activates macro-autophagy in several tissues, such as ovarian cancer cells, glioma cells, and skeletal muscle cells (Bock et al., 2010; Iovino et al., 2012). PED phosphorylation is important for its effect on macro-autophagy activation, since abrogation of PED phosphorylation strongly diminished the number of autophagic cells (Bock et al., 2010). Thus, it interesting to speculate that in cancer, CMA mainly targets unphosphorylated (tumor suppressive) PED, contributing in this way to chemo- or radio-therapy resistance.

Finally, phosphorylation status may regulate the level of PED also via other processes, such as ubiquitinylation and proteasomal targeting. Phorbol esters (12-*O*-tetradecanoylphorbol-13-acetate) increase PED expression at the post-translational level by inducing phosphorylation at

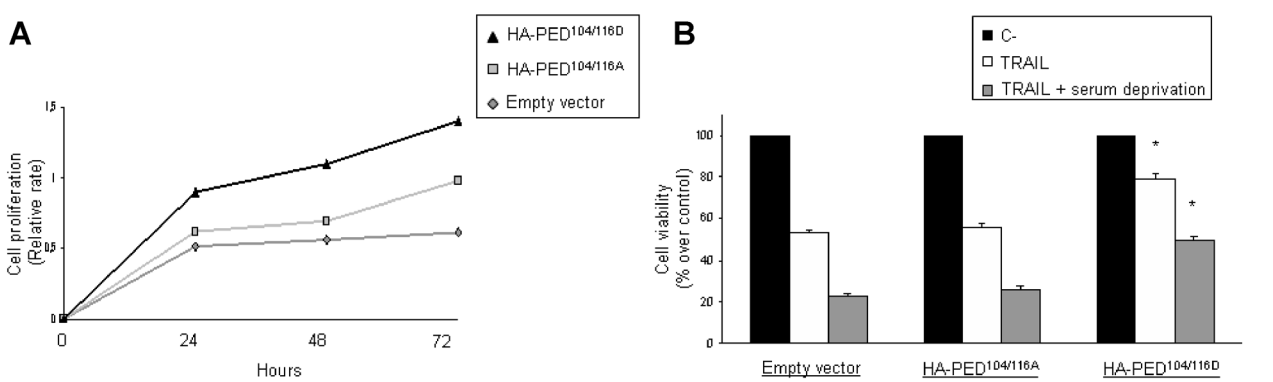

Fig. 6. Effect of PED phosphorylation on cell growth and apoptosis. A: A549 cells were transfected with either the phosphomimic or phosphorylation-dead mutant of PED. After 24 h, cells were serum-starved and cell viability assessed with an MTT assay at different time-points. B: A549 cells were transfected as indicated in A and after 24 h were treated with SuperKiller TRAIL (50 ng/ml), with or without serum deprivation for a further 24 h. Cell viability was assessed with an MTT assay. Means + SD. *$P < 0.028$ versus empty vector.

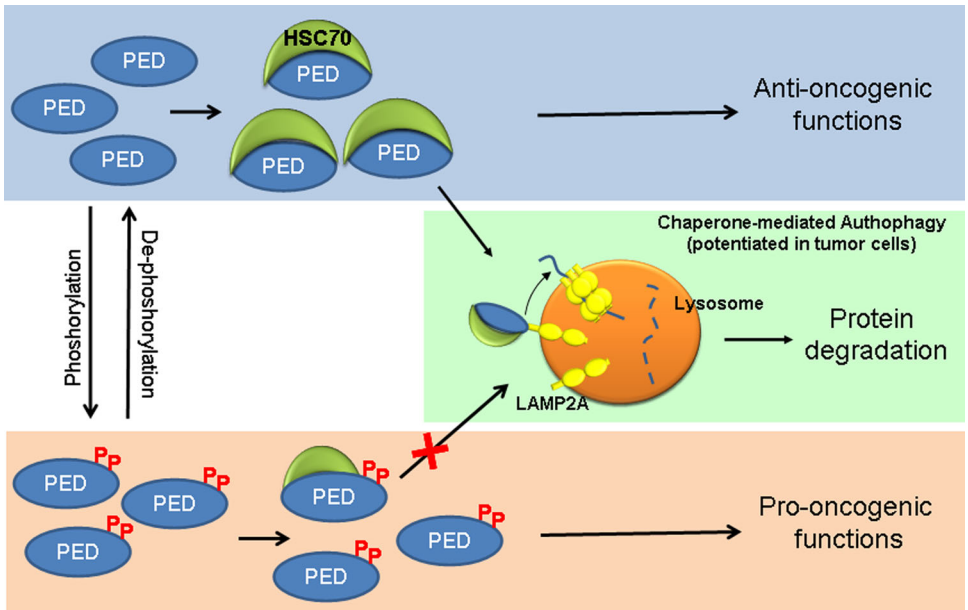

Fig. 7. Schematic of the modulation of phosphorylated (tumor promoter) and unphosphorylated (tumor suppressor) PED levels. Unphosphorylated PED binds HSC70, targeting it to degradation by chaperone-mediated autophagy. Within tumor cells, phosphorylated PED binds to HSC70 at reduced extent so as to preclude it generally from degradation. This results in an increase in the pro-tumoral/anti-apoptotic form of the protein.

Ser116 and preventing ubiquitinylation and proteosomal degradation (Perfetti et al., 2007). Thus, phosphorylation may be a general mechanism for the regulation of PED level, not only through CMA but also through the ubiquitin/proteasomal pathway.

Acknowledgments

We wish to thank Michael Latronico for carefully revising the manuscript and Anna Rienzo for technical help in confocal microscope images acquisition. This work was supported by Associazione Italiana Ricerca sul Cancro, AIRC to G.C. 10620 and 14046, MERIT to G.C. RBNE08E8CZ_002, POR Campania FSE 2007–2013 Project CRÈME to G.C., Fondazione Berlucchi to G.C., NIH/NIA AG031782 and AG03872 to A.M.C. C.Q. was supported by the "Federazione Italiana Ricerca sul Cancro" (FIRC) Post-Doctoral Research Fellowship and I.T. by a Fulbright Postdoctoral Fellowship.

Literature Cited

Bock BC, Tagscherer KE, Fassl A, Kramer A, Oehme I, Zentgraf H, Keith M, Roth W. 2010. The PEA-15 protein regulates autophagy via activation of JNK. J Biol Chem 285: 21644–21654

Condorelli G, Vigliotta G, Iavarone C, Caruso M, Tocchetti CG, Andreozzi F, Cafieri A, Tecce MF, Formisano P, Beguinot L, Beguinot F. 1998. PED/PEA-15 gene controls glucose transport and is overexpressed in type 2 diabetes mellitus. EMBO J 17:3858–3866

Condorelli G, Vigliotta G, Cafieri A, Trencia A, Andalo P, Oriente F, Miele C, Caruso M, Formisano P, Beguinot F. 1999. PED/PEA-15: an anti-apoptotic molecule that regulates FAS/TNFR1-induced apoptosis. Oncogene 18:4409–4415

Condorelli G, Trencia A, Vigliotta G, Perfetti A, Goglia U, Cassese A, Musti AM, Miele C, Santopietro S, Formisano P, Beguinot F. 2002. Multiple members of the mitogen-activated protein kinase family are necessary for PED/PEA-15 anti-apoptotic function. J Biol Chem 277:11013–11018

Cuervo AM, Dice JF. 2000. Regulation of lamp2a levels in the lysosomal membrane. Traffic 1:570–583

Cuervo AM, Terlecky SR, Dice JF, Knecht E. 1994. Selective binding and uptake of ribonuclease A and glyceraldehyde-3-phosphate dehydrogenase by isolated rat liver lysosomes. J Biol Chem 269:26374–26380

Cuervo AM, Dice JF, Knecht E. 1997. A population of rat liver lysosomes responsible for the selective uptake and degradation of cytosolic proteins. J Biol Chem 272:5606–5615

Dice JF 1990. Peptide sequences that target cytosolic proteins for lysosomal proteolysis. Trends Biochem Sci 15:305–309

Formstecher E, Ramos JW, Fauquet M, Calderwood DA, Hsieh J-C, Canton B, Nguyen X-T, Barnier J-V, Camonis J, Ginsberg MH, Chneiweiss H. 2001. PEA-15 mediates cytoplasmic sequestration of ERK MAP kinase. Dev Cell 1:239–250

Funke V, Lehmann-Koch J, Bickeböller MI , Benner A, Tagscherer KE, Grund K, Pfeifer M, Herpel E, Schirmacher P, Chang-Claude J, Brenner H, Hoffmeister M, Roth W. 2013. The PEA-15/PED protein regulates cellular survival and invasiveness in colorectal carcinomas. Cancer Lett 335:431–440

Garofalo M, Romano G, Quintavalle C, Romano MF, Chiurazzi F, Zanca C, Condorelli G. 2007. Selective inhibition of PED protein expression sensitizes B-cell chronic lymphocytic leukaemia cells to TRAIL-induced apoptosis. Int J Cancer 120:1215–1222

Garofalo M, Quintavalle C, Zanca C, De Rienzo A, Romano G, Acunzo M, Puca L, Incoronato M, Croce CM, Condorelli G. 2008. Akt regulates drug-induced cell death through Bcl-w downregulation. PLoS ONE 3:e4070

Hao C, Beguinot F, Condorelli G, Trencia A, Van Meir EG, Yong VW, Parney IF, Roa WH, Petruk KC. 2001. Induction and intracellular regulation of tumor necrosis factor-related apoptosis-inducing ligand (TRAIL) mediated apotosis in human malignant glioma cells. Cancer Res 61:1162–1170

Hayashi N, Peacock JW, Beraldi E, Zoubeidi A, Gleave ME, Ong CJ. 2012. Hsp27 silencing coordinately inhibits proliferation and promotes Fas-induced apoptosis by regulating the PEA-15 molecular switch. Cell Death Differ 19(6):990–1002doi:10.1038/cdd2011184 Epub 2011 Dec 16

Incoronato M, Garofalo M, Urso L, Romano G, Quintavalle C, Zanca C, Iaboni M, Nuovo G, Croce CM, Condorelli G. 2010. miR-212 increases tumor necrosis factor-related apoptosis-inducing ligand sensitivity in non-small cell lung cancer by targeting the antiapoptotic protein PED. Cancer Res 70:3638–3646

Incoronato M, Urso L, Portela A, Laukkanen MO, Soini Y, Quintavalle C, Keller S, Esteller M, Condorelli G. 2011. Epigenetic regulation of miR-212 expression in lung cancer. PLoS ONE 6:e27722

Iovino S, Oriente F, Botta G, Cabaro S, Iovane V, Paciello O, Viggiano D, Perruolo G, Formisano P, Beguinot F. 2012. PED/PEA-15 induces autophagy and mediates TGF-beta1 effect on muscle cell differentiation. Cell Death Differ 19:1127–1138

Kaushik S, Cuervo AM. 2009. Methods to monitor chaperone-mediated autophagy. Methods in Enzymology. New York: Academic Press; pp. 297–324

Kaushik S, Cuervo AM. 2012a. Chaperone-mediated autophagy: A unique way to enter the lysosome world. Trends Cell Biol 22:407–417

Kaushik S, Cuervo AM. 2012b. Chaperones in autophagy. Pharmacol Res 66:484–493

Kon M, Kiffin R, Koga H, Chapochnick J, Macian F, Varticovski L, Cuervo AM, Chaperone-mediated autophagy is required for tumor growth. Sci Transl Med 32011; 109ra117

Krueger J, Chou F-L, Glading A, Schaefer E, Ginsberg MH. 2005. Phosphorylation of phosphoprotein enriched in astrocytes (PEA-15) regulates extracellular signal-regulated kinase-dependent transcription and cell proliferation. Mol Biol Cell 16:3552–3561

Lee J, Bartholomeusz C, Krishnamurthy S, Liu P, Saso H, LaFortune TA, Hortobagyi GN, Ueno NT. 2012. PEA-15 unphosphorylated at both serine 104 and serine 116 inhibits ovarian cancer cell tumorigenicity and progression through blocking [beta]-catenin. Oncogenesis 1:e22

Lv L, Li D, Zhao D, Lin R, Chu Y, Zhang H, Zha Z, Liu Y, Li Z, Xu Y, Wang G, Huang Y, Xiong Y, Guan K-L, Lei Q-Y. 2011. Acetylation targets the M2 isoform of pyruvate kinase for degradation through chaperone-mediated autophagy and promotes tumor growth. Mol Cell 42:719–730

Majeski AE, Fred Dice J. 2004. Mechanisms of chaperone-mediated autophagy. Int J Biochem Cell Biol 36:2435–2444
Massey AC, Zhang C, Cuervo AM, Gerald S. 2006. Chaperone-mediated autophagy in aging and disease. Current topics in developmental biology. New York: Academic Press; pp. 205–235
Perfetti A, Oriente F, Iovino S, Alberobello AT, Barbagallo AP, Esposito I, Fiory F, Teperino R, Ungaro P, Miele C, Formisano P, Beguinot F. 2007. Phorbol esters induce intracellular accumulation of the anti-apoptotic protein PED/PEA-15 by preventing ubiquitinylation and proteasomal degradation. J Biol Chem 282:8648–8657
Renault F, Formstecher E, Callebaut I, Junier MP, Chneiweiss H. 2003. The multifunctional protein PEA-15 is involved in the control of apoptosis and cell cycle in astrocytes. Biochem Pharmacol 66:1581–1588
Romano G, Acunzo M, Garofalo M, Di Leva G, Cascione L, Zanca C, Bolon B, Condorelli G, Croce CM. 2012. MiR-494 is regulated by ERK1/2 and modulates TRAIL-induced apoptosis in non-small-cell lung cancer through BIM down-regulation. Proc Natl Acad Sci USA 109:16570–16575
Salvador N, Aguado C, Horst M, Knecht E. 2000. Import of a cytosolic protein into lysosomes by chaperone-mediated autophagy depends on its folding state. J Biol Chem 275:27447–27456
Stassi G, Garofalo M, Zerilli M, Ricci-Vitiani L, Zanca C, Todaro M, Aragona F, Limite G, Petrella G, Condorelli G. 2005. PED mediates AKT-dependent chemoresistance in human breast cancer cells. Cancer Res 65:6668–6675
Storrie B, Madden EA. 1990. Isolation of subcellular organelles. Methods Enzymol 182: 203–225
Sulzmaier FJ, Opoku-Ansah J, Ramos JW. 2012. Phosphorylation is the switch that turns PEA-15 from tumor suppressor to tumor promoter. Small GTPases 3:173–177
Trencia A, Perfetti A, Cassese A, Vigliotta G, Miele C, Oriente F, Santopietro S, Giacco F, Condorelli G, Formisano P, Beguinot F. 2003. Protein kinase B/Akt binds and phosphorylates PED/PEA-15, stabilizing its antiapoptotic action. Mol Cell Biol 23: 4511–4521
Zanca C, Garofalo M, Quintavalle C, Romano G, Acunzo M, Ragno P, Montuori N, Incoronato MR, Tornillo L, Baumhoer D, Briguori C, Terracciano L, Condorelli G. 2008. PED is overexpressed and mediates TRAIL resistance in human non-small cell lung cancer. J Cell Mol Med 225:63–72
Zanca C, Cozzolino F, Quintavalle C, Di Costanzo S, Ricci-Vitiani L, Santoriello M, Monti M, Pucci P, Condorelli G. 2010. PED regulates cell migration process in human Non Small Cell Lung Cancer cells through Rac1. J Cell Physiol 225:63–72

Supporting Information

Additional supporting information may be found in the online version of this article at the publisher's web-site.